Evidence for wavelength dependence of Xe *M*-shell emission from clusters

H. Honda
Center for Tsukuba Advanced Research Alliance, University of Tsukuba, 1-1-1 Tennodai, Tsukuba, Ibaraki 305-8577, Japan

E. Miura
Electrotechnical Laboratory, 1-1-4 Umezono, Tsukuba, Ibaraki 305-8568, Japan

K. Katsura, E. Takahashi, and K. Kondo
Center for Tsukuba Advanced Research Alliance, University of Tsukuba, 1-1-1 Tennodai, Tsukuba, Ibaraki 305-8577, Japan

(Received 27 April 1999; revised manuscript received 30 August 1999; published 7 January 2000)

X-ray yields of *M*-shell emission from Xe clusters excited by Ti:sapphire (800 nm) and KrF (248 nm) laser pulses were compared under the same irradiation condition that was experimentally well characterized. Xe clusters were irradiated by 350-fs laser pulses of 20-mJ energy. For the KrF laser irradiation, the absolute x-ray yield in the wavelength region from 8 Å to 16 Å was estimated to be 38 μJ per pulse. The x-ray yield was 20 times higher than that for the Ti:sapphire laser irradiation. It was found that the x-ray yield from clusters in the keV region depends on the pump laser wavelength.

PACS number(s): 36.40.Gk, 52.25.Nr, 52.50.Jm

The interaction of intense optical fields with clusters is of great interest. Ionization of a cluster and/or a diatomic molecule is completely different from that of an isolated atom and/or ion [1–7]. Anomalously highly charged ions were observed with clusters, although ionization of isolated atoms and/or ions can be followed by the Ammosov-Delone-Krainov (ADK) theory in the tunneling regime [8]. The difference could be attributed from the effect of the short distance between atoms which compose a cluster or a diatomic molecule. Then, it is important to study the interaction of intense optical fields with a diatomic molecule as the first step for understanding the mechanism of the anomalous ionization. Several experimental [6] and theoretical studies [7,9] have been reported for ionization of a diatomic molecule. On the other hand, it is important to study the interaction with a cluster and/or a large molecule for observing the enhanced and/or additional effects by the short distance between neighboring atoms. In addition to anomalous ionization, a large absorption of the laser energy at clusters was observed [10,11]. Recently, several groups reported the observation of fast ions of which kinetic energies reach $\sim$100 keV [4,5].

Previously, we reported that the keV x-ray yield from Xe clusters excited by a KrF laser was extremely larger than that by a Ti:sapphire laser [10,12]. However, in Ref. [13] they reported that the keV x-ray yield with a fundamental (ω) pulse of a Ti:sapphire laser was almost the same level as that with a second-harmonic (2ω) pulse. They described that the condition of the ω experiment was equal to that of the 2ω experiment, although there is no precise description of the condition of the 2ω experiment. In Ref. [14] a similar experimental result has also been reported. In our previous research the experimental conditions were not completely equal between the KrF and the Ti:sapphire experiments. To clarify the wavelength dependence of x-ray yields from clusters, we observed Xe *M*-shell emission by using Ti:sapphire (800 nm) and KrF (248 nm) laser systems under the same irradiation condition, which was experimentally well characterized.

In the KrF laser system, a frequency-tripled Ti:sapphire laser pulse operated at 745-nm wavelength was amplified with a discharge-pumped KrF laser. The energy of 20 mJ on target was obtained. The duration of a KrF laser pulse was measured by using a three-photon fluorescence technique [15]. A typical autocorrelation trace of a KrF laser pulse is shown in Fig. 1(a). The pulse duration was estimated to be 350 fs assuming the pulse shape of sech^2. The beam diameter of the KrF laser light was 50 mm. Since it was difficult to vary the energy and the pulse duration in the KrF laser system, we adjusted the operation condition of the Ti:sapphire laser system to that of the KrF laser system. The energy on target was set to 20 mJ by adjusting the pumping energy of the multipass amplifier. The pulse duration was set to 350 fs

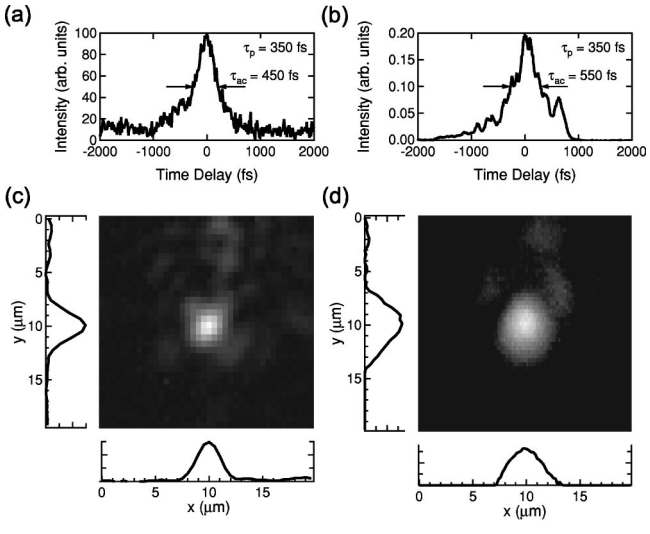

FIG. 1. Single-shot autocorrelation traces of (a) KrF and (b) Ti:sapphire laser pulses. The pulse durations τ_p were obtained by dividing the widths of the autocorrelation traces τ_{ac} by (a) 1.29 for the three-photon process and (b) 1.55 for the two-photon process, assuming the sech^2 pulse shape. Focal spot patterns of (c) KrF and (d) Ti:sapphire lasers in vacuum.

by adjusting the distance between two gratings in the pulse compressor. A typical autocorrelation trace of a Ti:sapphire laser pulse observed with a single-shot autocorrelator using the two-photon process is shown in Fig. 1(b). To achieve the same focusing condition of $f/3$, the final beam diameter was set to 50 mm. The laser beam was focused with an off-axis parabolic mirror of 165 mm in focal length in both experiments. The focal spot patterns in vacuum recorded on charge-coupled device (CCD) cameras and their spatial profiles are shown in Figs. 1(c) and 1(d). Spatial resolutions for the KrF and Ti:sapphire lasers were estimated to be 1.5 and 2.4 μm, respectively. As seen in Figs. 1(c) and 1(d), the spot diameters for KrF and Ti:sapphire laser beams were 3 and 4 μm in full width at half maximum (FWHM), respectively.

Xe gas jets containing clusters were irradiated by the KrF and Ti:sapphire lasers under the same condition as described below. Xe clusters were injected into vacuum from a pulsed valve with an orifice of 2 mm in diameter. The laser light was focused 2 mm below the orifice. The typical backing pressure of the pulsed valve was 8.5 bar, which corresponds to the cluster size of 2.9×10^6 calculated from the empirical formula given by Hagena [16,17]. The average atomic density of the Xe gas jet was measured to be 5×10^{18} cm^{-3} around the focal point by an interferometric technique [18]. Because the identical pulsed valve was used in both experiments, the spatial density distributions were equal around the focal point.

To achieve the same irradiation condition, a prepulse level was reduced by optimizing operation condition of laser systems. In both laser systems, the contrast ratio of the regenerative amplifier was optimized. To confirm no preformed plasma, time-resolved shadowgraphs of a plasma filament were observed. As a probe pulse, we used an unconverted pulse from nonlinear crystals for the third-harmonic generation in the KrF laser system and a pulse partially split from a pump beam in the Ti-sapphire laser system, respectively. The pulse durations of the probe pulses were 130 and 350 fs for the KrF and Ti:sapphire experiments, respectively. The probe pulse was incident transverse to the propagation direction of the pump beam. By adjusting the time delay between the probe and the pump pulses, time-resolved shadowgraphs of plasma filaments were recorded on a CCD camera. Figure 2 shows typical images of a plasma filament for KrF and Ti:sapphire laser irradiation. These images were observed a few ps before the arrival of the pump pulse at the focal point. As seen in Figs. 2(a) and 2(b), we confirmed that no preformed plasma was produced for both KrF and Ti:sapphire laser irradiation. In the KrF laser system, it was confirmed that the plasma was not produced by the amplified spontaneous emission from the discharge amplifier.

An x-ray spectrum in the keV region was recorded on a Kodak DEF film through a 1.6-μm-thick Al filter with a potassium acid phthalate ($KHC_8H_4O_4$, KAP) crystal. The x-ray crystal spectrometer was placed transverse to the direction of the laser propagation. The spectral resolution was estimated to be 0.07 Å. The optical density of the film was converted to the x-ray intensity by using the characteristic curve calibrated by Henke and co-workers [19]. The spectral

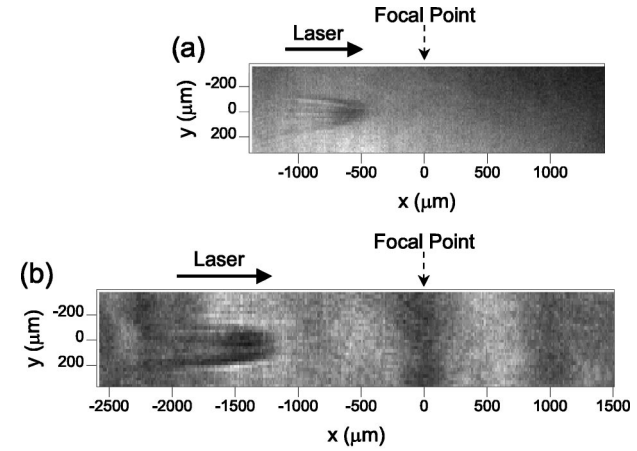

FIG. 2. Time-resolved shadowgraphs of a plasma filament generated by the laser pulse propagating in the Xe gas jet. The laser pulses propagate from the left to the right. The focal points in the shadowgraphs are at $x=0$ μm, which was determined from the shadowgraphs taken at the time when the pump pulse arrived at the focal point. No preformed plasma generated by a prepulse was confirmed for both (a) KrF and (b) Ti:sapphire laser irradiation. These images were observed (a) 1.4 ps and (b) 3.9 ps before the arrival of the pump pulse at the focal point.

responses of the filter transmission and the integrated reflectivity of the crystal were estimated by using the mass absorption coefficient and the theoretical value based on the Darwin-Prins model reported in Ref. [20]. The identical spectrometer was used in both experiments. X-ray images in the keV region were recorded on a CCD camera through a 1.6-μm Al filter with a pinhole of 25 μm in diameter for KrF laser irradiation and 50 μm for Ti:sapphire laser irradiation. The x-ray pinhole camera was placed transverse to the direction of the laser propagation.

The absolute x-ray spectra are shown in Fig. 3. The thick and the thin lines represent the x-ray spectra for the KrF and

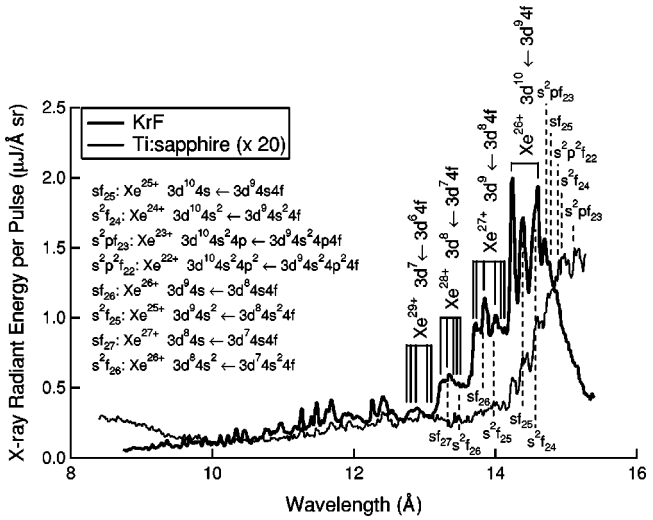

FIG. 3. Comparative Xe *M*-shell spectra observed for KrF (thick line) and Ti:sapphire (thin line) laser irradiation. The ordinate of the thin line is increased by a factor of 20.

Ti:sapphire laser irradiation, respectively. The ordinate of the thin line is increased by a factor of 20 in order to enhance the visibility of the spectrum. Assuming the uniform angular distribution into 4π steradian, the yields of *M*-shell emission in the wavelength region from 8 to 16 Å were estimated to be 38 and 1.5 μJ per pulse for KrF and Ti:sapphire laser irradiation, respectively. The x-ray yield for the KrF laser irradiation was 20 times higher than that for the Ti:sapphire laser irradiation. After the calculation of the wavelength from the geometry of the spectrometer, the line assignment was carried out by comparing the calculation with the results reported in Ref. [21]. As seen in Fig. 3, lines from Xe^{26+} to Xe^{29+} ions were observed in the spectrum for the KrF laser irradiation. In contrast, for the Ti:sapphire laser irradiation, although lines from Xe^{26+} ions were observed, lines from Xe^{27+} to Xe^{29+} ions were weak. In the wavelength region longer than 15 Å, the bump of the spectrum for the Ti:sapphire laser irradiation can been seen. According to the line assignment reported in Ref. [21], the existence of lines from Xe^{23+} to Xe^{25+} ions has been pointed out in this wavelength region. It is clear that the charge states of Xe ions for the KrF laser irradiation were higher than those for the Ti:sapphire laser irradiation. The higher charge state for the KrF laser irradiation may bring about the higher x-ray yield in the keV region.

Figure 4 shows x-ray images observed with an x-ray pinhole camera. As seen in Fig. 4, it was found that the lengths of the x-ray emitting regions were much longer than the Rayleigh lengths of 80 and 45 μm for KrF and Ti:sapphire laser irradiation. In addition, the x-ray emitting regions were not limited around the focal point in both cases. In our experiment, the peak intensities in vacuum were estimated to be 8×10^{17} W/cm^2 and 4×10^{17} W/cm^2 for KrF and Ti:sapphire laser irradiation, respectively. However, the difference of the peak intensities do not affect total x-ray yields.

In experiments using the Ti:sapphire laser system, we measured x-ray yields of Xe *M*-shell emission by changing the laser energy and the pulse duration. When the pulse duration was set to 350 fs, the x-ray yield for 40-mJ energy was three times higher than that for 20 mJ. When the laser energy was set to 40 mJ, the x-ray yield for 150-fs pulse duration was two times higher than that for 350 fs. In Ref. [10], the x-ray yield of Xe *M*-shell emission for KrF laser irradiation was 100 times higher than that for Ti:sapphire laser irradiation. In that experiment, the laser energy and the pulse duration were 220 mJ and 270 fs in the KrF laser. In contrast, the laser energy and the pulse duration were 50 mJ and 90 fs in the Ti:sapphire laser. Considering the dependence of the x-ray yield on the laser energy and the pulse duration described above, the large difference of x-ray yields between KrF and Ti:sapphire laser irradiation could be understood.

The following experimental result has been reported in Ref. [13]. When the same size Kr clusters were irradiated by fundamental (ω) and second harmonic (2ω) pulses of a Ti:sapphire laser (790 nm) at the same laser intensity, the x-ray yield of Kr *L*-shell emission for the 2ω pulse irradiation was comparable to that for the ω pulse irradiation. Because the difference of wavelengths is smaller than that in our case, the difference of x-ray yields between the ω and

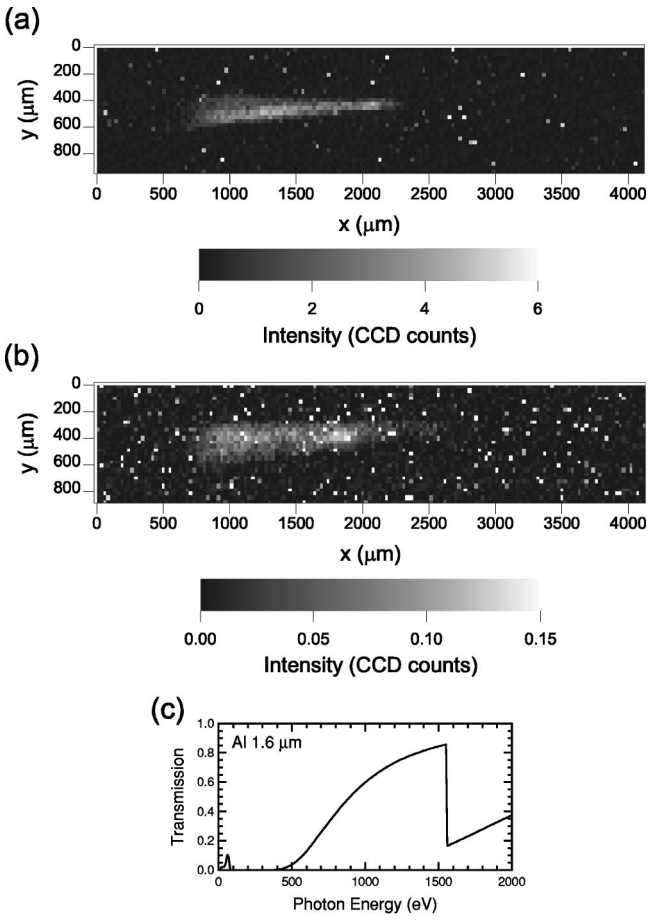

FIG. 4. X-ray pinhole camera images through a 1.6-μm Al filter for (a) KrF and (b) Ti:sapphire laser irradiation. The pinhole diameters were 25 and 50 μm for (a) KrF and (b) Ti:sapphire laser irradiation, respectively. The intensity scales of the images are shown under each image. The difference of pinhole diameters was taken into account in these scales. (c) Transmission of a 1.6-μm Al filter.

the 2ω pulses is expected to be smaller than that in our case. It should be noted that duration of the 2ω pulse may be longer than that of the ω pulse owing to the group velocity mismatch in a nonlinear crystal. However, there is no detailed description of the experimental condition of 2ω pulse irradiation. As seen in our experimental results for the Ti:sapphire laser, even if the laser energies were equal, the longer pulse gave the lower x-ray yield. Thus, we think that the longer duration of the 2ω pulse led to the same level x-ray yields for ω and 2ω pulse irradiation.

Several theoretical models have been proposed to explain high charge states and strong x rays from clusters irradiated by an intense laser pulse [17,22,23]. Rhodes and co-workers have explained high charge states in clusters by considering the coherent motion of multielectrons [22]. According to this model, the approximated number of ionization events N_x' is given by Eq. (1) [22],

$$N_x' \propto n^{4/3}\left(\frac{2\tau c Z^2 \sigma_{ei}}{\lambda r_0^2}\right). \tag{1}$$

In Eq. (1), n, τ, c, Z, σ_{ei}, r_0, and λ are the number of atoms in the cluster, the interaction time, the light velocity, the ionic charge, the inelastic electron impact ionization cross section, the interatomic spacing, and the laser wavelength, respectively. As seen in Eq. (1), it is clear that more ionization events are given by the shorter-wavelength laser. Then, the higher x-ray yields are obtained with the shorter-wavelength laser.

Ditmire and co-workers have proposed the model that a microplasma is heated by the inverse bremsstrahlung [17]. In Ref. [17] the heating rate of the microplasma $\partial U/\partial t$ is given by Eq. (2),

$$\frac{\partial U}{\partial t}=\frac{9\omega^2\omega_p^2\nu}{8\pi}\frac{1}{9\omega^2(\omega^2+\nu^2)+\omega_p^2(\omega_p^2-6\omega^2)}|E_0|^2. \quad (2)$$

In Eq. (2), ω, ω_p, ν, and E_0 are the frequency of laser light, the plasma frequency, the electron-ion collision frequency, and the electric field in vacuum, respectively. The local atomic density in clusters is estimated to be 1.2×10^{22} cm^{-3} from the nearest Xe interatomic distance of 4.4 Å. After achieving high charge state, the electron densities of the microplasmas become much higher than the critical densities of both lasers. Therefore, ω_p is higher than ω. In addition, ν is assumed to be comparable to ω as reported in Ref. [17]. Then, Eq. (2) is approximated as follows:

$$\frac{\partial U}{\partial t}\cong\frac{9\nu}{8\pi}\left(\frac{\omega}{\omega_p}\right)^2|E_0|^2. \quad (3)$$

As seen in Eq. (3), the shorter-wavelength laser gives the larger heating rate. The higher temperature given by the larger heating rate leads to the higher x-ray yields. Thus, we conclude that x-ray yields from clusters depend on the wavelength of the pump laser. However, to discuss more precisely, the simulation reported in Ref. [17] is required because the strong variation of the electron density due to Coulomb explosion should be considered.

In conclusion, it is demonstrated that the x-ray yield in the keV region from clusters strongly depends on the wavelength of the pump laser by comparing *M*-shell emission from Xe clusters excited by infrared and ultraviolet laser pulses. The x-ray yield of Xe *M*-shell emission for the KrF laser irradiation was 20 times higher than that for the Ti:sapphire laser irradiation. The significant difference of x-ray spectra was observed. The higher ionization state for the KrF laser irradiation seemed to bring about the higher x-ray yield.

We would like to acknowledge the suggestion on operating the KrF laser system by Dr. S. Szatmári. This work was supported by the Research Foundation for Opto-Science and Technology, the University of Tsukuba Research Projects, and the University of Tsukuba TARA project.

[1] A. McPherson, T. S. Luk, B. D. Thompson, A. B. Borisov, O. B. Shiryaev, X. Chen, K. Boyer, and C. K. Rhodes, Phys. Rev. Lett. **72**, 1810 (1994); A. McPherson, B. D. Thompson, A. B. Borisov, K. Boyer, and C. K. Rhodes, Nature (London) **370**, 631 (1994).

[2] T. Ditmire, T. Donnelly, R. W. Falcone, and M. D. Perry, Phys. Rev. Lett. **75**, 3122 (1995).

[3] E. M. Snyder, S. A. Buzza, and A. W. Castleman, Jr., Phys. Rev. Lett. **77**, 3347 (1996).

[4] T. Ditmire, J. W. G. Tisch, E. Springate, M. B. Mason, H. Hay, R. A. Smith, J. Marangos, and M. H. R. Hutchinson, Nature (London) **386**, 54 (1997).

[5] M. Lezius, S. Dobosz, D. Normand, and M. Schmidt, Phys. Rev. Lett. **80**, 261 (1998).

[6] D. T. Strickland, Y. Beaudoin, P. Dietrich, and P. B. Corkum, Phys. Rev. Lett. **68**, 2755 (1992).

[7] T. Seideman, M. Yu. Ivanov, and P. B. Corkum, Phys. Rev. Lett. **75**, 2819 (1995).

[8] M. V. Ammosov, N. B. Delone, and V. P. Krainov, Zh. Éksp. Teor. Fiz. **91**, 2008 (1986) [Sov. Phys. JETP **64**, 1191 (1986)].

[9] G. N. Gibson, G. Dunne, and K. J. Bergquist, Phys. Rev. Lett. **81**, 2663 (1998).

[10] K. Kondo, A. B. Borisov, C. Jordan, A. McPherson, W. A. Schroeder, K. Boyer, and C. K. Rhodes, J. Phys. B **30**, 2707 (1997).

[11] T. Ditmire, R. A. Smith, J. W. G. Tisch, and M. H. R. Hutchinson, Phys. Rev. Lett. **78**, 3121 (1997).

[12] W. A. Schroeder, F. G. Omenetto, A. B. Borisov, J. W. Longworth, A. McPherson, C. Jordan, K. Boyer, K. Kondo, and C. K. Rhodes, J. Phys. B **31**, 5031 (1998).

[13] S. Dobosz, M. Lezius, M. Schmidt, P. Meynadier, M. Perdrix, D. Normand, J. P. Rozet, and D. Vernhet, Phys. Rev. A **56**, R2526 (1997).

[14] T. Ditmire, P. K. Patel, R. A. Smith, J. S. Wark, S. J. Rose, D. Milathianaki, R. S. Marjoribanks, and M. H. R. Hutchinson, J. Phys. B **31**, 2825 (1998).

[15] N. Sarukura, M. Watanabe, A. Endoh, and S. Watanabe, Opt. Lett. **13**, 996 (1988).

[16] O. F. Hagena, Rev. Sci. Instrum. **63**, 2374 (1992).

[17] T. Ditmire, T. Donnelly, A. M. Rubenchik, R. W. Falcone, and M. D. Perry, Phys. Rev. A **53**, 3379 (1996).

[18] K. Kondo, H. Suzuki, L. B. Sharma, A. B. Borisov, K. Boyer, and C. K. Rhodes (unpublished).

[19] B. L. Henke, J. Y. Uejio, G. F. Stone, C. H. Dittmore, and F. G. Fujiwara, J. Opt. Soc. Am. B **3**, 1540 (1986).

[20] B. L. Henke, E. M. Gullikson, and J. C. Davis, At. Data Nucl. Data Tables **54**, 181 (1993).

[21] A. B. Borisov, J. W. Longworth, A. McPherson, K. Boyer, and C. K. Rhodes, J. Phys. B **29**, 247 (1996).

[22] K. Boyer, B. D. Thompson, A. McPherson, and C. K. Rhodes, J. Phys. B **27**, 4373 (1994).

[23] C. Rose-Petruck, K. J. Schafer, K. R. Wilson, and C. P. J. Barty, Phys. Rev. A **55**, 1182 (1997).